Electrochemical sensing of anti-cancer drug (Capecitabine) by GC-MWCNT-PAMAM (G3)-AuNps electrode

Eagambaram Murugan*, Chennakesavapuram R Akshata, Annie Stephy

Department of Physical Chemistry, School of Chemical Sciences, University of Madras, Guindy Campus, Guindy, Chennai- 600025, Tamil Nadu, India

*Corresponding author, E-mail: dr.e.murugan@gmail.com; Tel: (+91) 9444275889

Received: 02 April 2016, Revised: 10 August 2016 and Accepted: 20 December 2016

DOI: 10.5185/amp.2017/309
www.vbripress.com/amp

Abstract

Capecitabine (CPT) is an oral antineoplastic prodrug of 5-Flurorouracil (5-FU), administered for the treatment of metastatic breast and colorectal cancers. Detection of trace quantity of Capecitabine in pharmaceutical drug dosages is very crucial and essential owing to its life threating toxic adverse effects. In this study, an effective conducting nanohybrid namely, MWCNT-PAMAM (G3)-AuNps was developed and characterized by Raman, FT-IR, SEM and HR-TEM techniques. The developed conducting nanohybrid was used for fabrication of effective and stable active electrode viz., GCE-MWCNT-PAMAM (G3)-AuNps which in turn demonstrated for effective sensing of trace quantity of Capecitabine i.e., at a concentration of 5×10^{-12} M under lower potentials. The reduction of Capecitabine was investigated through cyclic voltammetry in the presence of H_2SO_4 (pH 1.54) as supporting electrolyte. The presence of Capecitabine exhibited an irreversible reductive peak potential at ~0.835 V which was observed from mixed diffusion-adsorption controlled processes. The mechanism for electrochemical-chemical reduction, trace and rapid determination of Capecitabine are reported. This newly developed electrode has a potential to sense/ detect the Capecitabine at the concentration of 5×10^{-12} M under lower potentials. Further, it is expected that there is a strong scope for quality control in pharmaceutical formulates. Copyright © 2017 VBRI Press.

Keywords: Capecitabine, 5-Flurorouracil, Poly (amidoamine), multiwalled carbon nanotube, gold nanoparticles, electrochemical sensing.

Introduction

In the current scenario, it is reported that cancer is a leading cause for death which accounts for about 8.2 million cases of deaths globally (World Cancer Report). Its mortality rate has been increasing at an alarming rate. Hence, various anti-cancer agents have been designed and clinically evaluated by Government and Pharmaceutical industries to combat and eradicate this issue. Among the various treatments being practiced by oncologists, Capecitabine, a fluoropyrimidine carbamate is orally administrated chemotherapeutic prodrug of 5-Flurorouracil (5-FU) which is used for the treatment of metastatic breast cancer and colorectal cancer. It is reported that 5-FU is a fluorinated analog of uracil [**1**], which inhibits the *de novo* thymidine synthesis and prevents DNA synthesis and ultimately leading to cancerous cell death. Chemically, Capecitabine is 5'-deoxy-5-fluoro-N-[(pentyloxy) carbonyl]-cytidine. Capecitabine drug is approved to use as a single agent (monotherapy) [**2]** or in combination therapy [**3,4**]. Capecitabine is preferentially converted by tumour-selective mechanism via three step enzymatic cascade with higher concentrations of 5-FU in malignant cells as compared with normal tissues [**5, 6**]. Although Capecitabine has greater therapeutic efficacy but the drug has proved to cause life threating toxicities which comprises of neurotoxicity [**7**], cardiotoxicity [**8**], gastrointestinal toxicity, dermotological toxicity, hematological imbalance [**9**] and also other manifestations include dermatological hand and foot syndrome [**10**], diarrhea and hepatic hyperbilirubinemia [**11**]. Therefore, due to its severe toxicity, determination of its accurate concentration in pharmaceutical dosages and biological fluids is very much essential and thus gained greater significance in drug quality control.

So far, various analytical methods have been demonstrated for the determination of Capecitabine drug, which includes chromatography, spectrophotometry and spectroscopy [**12-16**]. But, these methods witness their own major setbacks which inclusive of tedious, time consuming and expensive in trace quantity determination. Alternatively, in the recent days, it is observed that electrochemical methods have gained much popularity and has extensively applied for quantitative trace determination of biomolecules [**17**] and drugs like antibiotic [**18**], antidiabetic [**19**],

antihypertensive [**20**], anticancer [**21, 22**] etc. Electrochemical technique is an elegant, simple and sensitive method used for rapid trace determination of analytes. In addition, electrochemical method furnishes deeper insight into the metabolic fate of the drug in the biological system.

Carbon nanotubes (CNTs) have been generating an immense research interest since discovery [**23**] owing to their unique mechanical, electrical, optical, chemical and thermal properties and as well as larger surface area. Hence, CNT has been extensively used in several applications such as sensor [**24**], nano-electronics [**25**], drug delivery [**26**], biomedical imaging [**27**] etc. Rolling up of the single or multiple graphene sheet(s) into cylinder produces single walled carbon nanotube (SWCNT) or multi-walled carbon nanotube (MWCNT) respectively. However, practical usage of MWCNT has been restricted due to poor solubility in water and organic solvents. Therefore, functionalization of MWCNTs is an ideal approach to enhance its solubility and at the same time preserving its electronic and mechanical parameters. In the present study, the pristine MWCNT was oxidized using low molecular weight phase transfer catalyst namely tetrabutyl ammonium bromide (TBAB) and potassium permanganate ($KMnO_4$) as mild oxidizing agents [**28,29**] in order to retain intact electronic and mechanical properties, which are the key motive of functionalizing MWCNTs. Further, functionalization of CNT by polymeric molecules like dendrimer has proven to be an efficient strategy for accomplishing better solubility [**30**]. Dendrimers are highly branched three-dimensional polymeric macromolecules [**31**] which are widely used in electrochemical determination. In this study, dendrimer Poly (amidoamine) (PAMAM) of generation level three [PAMAM (G3)] was chosen for MWCNT functionalization by taking into the facts that (i) lower generation level dendrimer cannot provide sufficient surface area for nanoparticle encapsulation and (ii) while the higher generation level dendrimer decreases the surface area by stearic hindrance. Therefore, intermediate level having generation 3 of PAMAM dendrimer are expected to provide abundant surface functional groups which in turn enable for more nanoparticle entrapment. Gold nanoparticles (AuNps) were chosen in this study because of its exceptional electrical, optical and catalytic properties. It is well established fact that aggregations of metal nanoparticles leads to diminish its electroactive surface area. Hence, for higher electrocatalytic activity, fine dispersion of metal nanoparticles is desirable. The prevention of metal nanoparticles aggregation was observed by entrapment of nanoparticles into the cavities of PAMAM dendrimer and thus stabilized. Sutriyo and co-workers used PAMAM (G4) as a stabilizing agent for gold nanoparticles [**32**]. PAMAM (G3) stabilized gold nanoparticles in turn provides higher electrocatalytic activity as a result of well dispersion of nanoparticles rather than aggregation and hence accounting for excellent electrocatalytic activity of the nanohybrid. The covalent conjugation of MWCNTs and PAMAM (G4) was reported for electrochemical determination of paracetamol [**33**]. Similarly, Glassy carbon electrode modified MWCNT-PAMAM complex was employed for biosensing of glycans [**34**].

To the best of our knowledge, few reports are available for electrochemical detection of Capecitabine at unmodified glassy carbon electrode (GCE) [**35**]. Hence, in the present study, we developed a new efficient GC modified electrode for trace/negligible quantity determination of Capecitabine. That is, synthesis of an effective conducting nanohybrid via integration of three smart materials namely MWCNT, dendrimer and metal nanoparticles by (i) fabrication of MWCNT-PAMAM (G3)-AuNps on GCE to produce stable active efficient GC-MWCNT-PAMAM (G3)-AuNps electrode and (ii) the newly developed nanohybrid coated electrode was used to determine the trace/negligible quantity of Capecitabine drug using cyclic voltammetry.

Experimental

Materials

Multi-Walled Carbon Nanotubes (MWCNT) diameter 140 nm [95%, Sisco Laboratory Research (SRL)], Poly (amidoamine) dendrimer of generation 3 [PAMAM (G3), Sigma-Aldrich], Dichloromethane (99%, SRL), Gold(III) chloride Trihydrate (≥ 99.9%, Sigma-Aldrich), Tetra-n-butylammonium bromide (≥ 98.0%, Sigma-Aldrich), N-(3-Dimethylamino - propyl)-N′-ethylcarbodiimide hydrochloride (EDC, 99%, Sigma-Aldrich), N-Hydroxysuccinimide (NHS, 98%, Sigma-Aldrich), Potassium permanganate ($KMnO_4$, Ranbaxy), Sodium borohydride (95%, SRL), Sulphuric acid (H_2SO_4, Merck), Boric acid (CDH), Phosphoric acid, Acetic acid (99.9%, SRL), Ethanol, Sodium hydroxide (NaOH, SRL) and Sodium acetate (Rankem). All reagents were analytical grade and used as obtained.

Instrumentation

Electrochemical measurements were executed using CHI 1130A electrochemical workstation (USA). A three-electrode system composed of a glassy carbon as a working electrode (φ = 3 mm), Ag/AgCl as a reference electrode, and platinum electrode as a counter electrode were used. All measurements were carried out at room temperature. Ultrasonication was performed by Cole Palmer sonication bath. Fourier transform-infrared spectra of the sample ground with KBr pellet were recorded on Bruker Tensor-27 FT-IR Spectrophotometer with OPUS software. Raman spectra were recorded using a Confocal Raman Instrument (Raman I-11 model), Nanophoton corporation, Japan, at room temperature using Argon

ion laser source (20mW) with wavelength of 532 nm. The surface morphology of the nanohybrids was analyzed with FESEM and the images were recorded using HITACHI SU 6600 field emission-scanning electron microscope (FESEM) and High-resolution transmission electron microscopy (HRTEM) analysis was also performed on JEOL 3010 transmission electron microscope instrument operating at 200 kV. The sample under analysis was ultrasonicated with ethanol for a 10 min and drop-cast onto a glow-discharged carbon-coated grid and followed by evaporation of the solvent to record better HR-TEM, image.

Oxidation of multi-walled carbon nanotubes

Initially, 0.05g of pristine MWCNT was added to 15 mL of dichloromethane taken in a 100 mL round bottomed flask and the mixture was thoroughly dispersed by Ultrasonication for 10 min. Later, 0.25 g (1.097 mmol) of TBAB dissolved in 5 mL water, 0.065 g of $KMnO_4$ dissolved in 5 mL water and 5 mL of acetic acid were added to the reaction flask. Thereafter, the mixture was refluxed with magnetic stirring at 80°C for 48 h (Scheme-1, step-I) and then the reaction mixture was diluted with addition of 200 mL of deionized water in order to get rid of the unreacted components, this process was repeated for another four cycles. The resulting solution containing oxidized MWCNT was subjected to centrifugal sedimentation and washed with deionized water up to the pH of the filtrate reached neutral (at least 10 cycles were required). After vacuum drying the filtrate, black colour powder of carboxyl/hydroxyl group functionalized multi-walled carbon nanotube namely, MWCNT-COOH/OH was obtained.

Functionalization of Poly (amidoamine) dendrimers PAMAM (G3) on MWCNT-COOH/OH

Initially, 0.020 g of MWCNT-COOH/OH hybrid was taken in a 50 mL round-bottom flask equipped with nitrogen protection and it was dispersed in 10 mL water. To this, 10 mg of EDC dissolved in 5mL of deionized water, 10mg of NHS dissolved in 5mL of deionized water, 30 mg of poly (amidoamine) dendrimer [PAMAM (G3)] was added and the mixture was stirred for 24 h, at room temperature (**Scheme 1**, step II). The resulting mixture containing PAMAM (G3) functionalized MWCNT-COOH/OH was subjected to high speed centrifugal sedimentation and thus produced black solution. The resulting solution was dried in vacuum oven at 80°C for 24 h to produce black colour powder of PAMAM (G3) dendrimer functionalized multiwalled carbon nanotubes [MWCNT-PAMAM (G3)].

Encapsulation of MWCNT-PAMAM (G3) with Gold nanoparticle

In step-III encapsulation of Gold nanoparticles was carried out. That is, 10 mg of MWCNT-PAMAM (G3) were taken and dispersed in 20 mL of deionized water. Then 0.05g (12mmol) of $HAuCl_4$ was dissolved in 10 mL of deionized water and added to the above solution. The resulting mixture was then stirred for 3 h at room temperature. To this, a freshly prepared $NaBH_4$ solution was added dropwise and then stirring was continued for another 16 h to ensure the complete reduction of Au^{3+}. Finally, the resulting product was centrifuged and washed repeated for three times, then dried at 80°C under vacuum for 12 h, and thus gold nanoparticles immobilized conducting nanohybrid in the form of powder with black colour was obtained and labeled as MWCNT-PAMAM (G3)-AuNps (Scheme 1, step III).

Fabrication of stable and efficient electrode namely GCE-MWCNT-PAMAM (G3)-AuNps

Prior to the fabrication, the bare GCE was selected as a working electrode and it was initially polished with 0.5-μm alumina powders on a polishing cloth (Buehler) in order to enhance the sensitivity of the voltammetric peaks and subsequently washed with ethanol and distilled water through ultrasonication and dried at room temperature. A stock solution of MWCNT-PAMAM (G3)-AuNps was prepared separately by dispersing 0.5 mg of nanohybrid in 500 μL deionized water and the sample was sonicated for 5 minutes. The aliquot of the same having 10 μL was taken and coated onto pretreated GCE which was allowed to air dry at room temperature. Subsequently, the resulting fabricated GCE-MWCNT-PAMAM (G3)-AuNps electrode was immersed in 0.5 M H_2SO_4 (pH 1.54) supporting electrolyte and was used for electrochemical investigations by cyclic voltammetry.

Scheme 1. Schematic representation of the synthesis of MWCNT-PAMAM (G3)-AuNps nanohybrids by oxidation (step-I), functionalization with PAMAM (G3) dendrimer (step-II) and encapsulation with gold nanoparticles (step III).

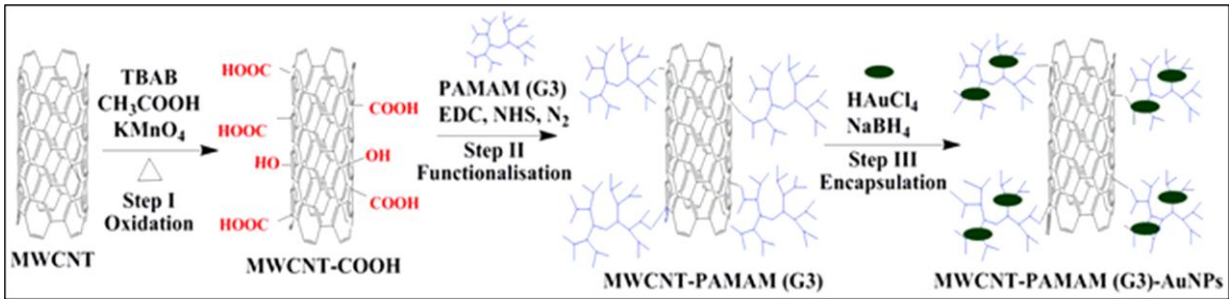

Results and discussion

FT-IR studies

The substantial evidence for chemical oxidation of MWCNT, functionalization of PAMAM (G3) dendrimer onto MWCNT-COOH/OH and deposition of gold nanoparticle onto the surface of MWCNT-PAMAM (G3)-AuNps was confirmed by FT-IR. The FT-IR spectra of the pristine MWCNT, MWCNT-COOH and MWCNT-PAMAM (G3) are shown in **Fig. 1**. The spectrum of pristine MWCNT in **Fig. 1(a)** has displayed a low intensity characteristic peak at 2953 cm^{-1} which are assigned for stretching vibration of C-H group and the peak noticed at 1632 cm^{-1} was attributed to stretching vibration of C=C group. Whereas, the spectrum for MWCNT-COOH in Fig. 1b has displayed the appearance of an absorption band at 1723 cm^{-1} which attributed to C=O stretching vibrations of carboxyl group [**36**]. The peak observed at 3000 cm^{-1} was assigned to the O-H stretching vibrational modes of the terminal carboxyl and carbonyl groups. The MWCNT-PAMAM (G3) spectrum in Fig. 1c showed the presence of the band at 3506 cm^{-1} which is attributed to N-H stretching vibration of terminal $–NH_2$. The appearance of the peaks at 1646 cm^{-1} and 1457 cm^{-1} was due to the stretching of carbonyl group of amide (-CO-NH) and the disappearance of C=O stretching vibrations at 1723 cm^{-1} established the fact that the -COOH group were transformed to -CO-NH amide group [**37**]. The obtained cumulative FT-IR results provide the evidence for functionalization of -COOH and PAMAM (G3) on MWCNT.

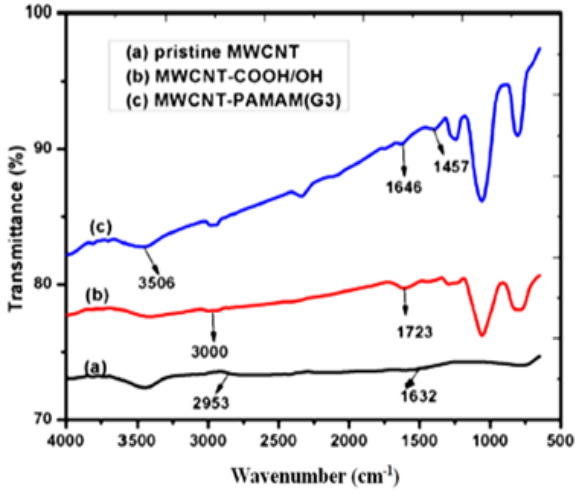

Fig. 1. The FT-IR spectra of (a) pristine MWCNT, (b) MWCNT-COOH/OH and (c) MWCNT-PAMAM (G3)

Raman Studies

Raman spectroscopy is very crucial technique to evaluate the quantum of –COOH/OH and PAMAM(G3) dendrimer molecules functionalized on MWCNT. The Raman spectra of pristine MWCNT, MWCNT-COOH, MWCNT-PAMAM (G3) and MWCNT-PAMAM (G3)-AuNps are shown in **Fig. 2**. The tangential G-band was observed at 1576 cm^{-1} which are associated with the ordered sp^2 hybridized carbon. While, the band observed at 1343 cm^{-1} was due to disorder induced D-band which are associated with the disordered sp^3 hybridized carbon [**38**]. Gururaj and coworkers carried out analog work of grafting PAMAM (G4) onto MWCNT [**39**]. The observed I_D/I_G ratio is found to increase proportionately to the functionalization of –COOH/OH and PAMAM (G3) dendrimer molecules. In other words, the I_D/I_G values for MWCNT-COOH, MWCNT-PAMAM (G3) and MWCNT-PAMAM (G3)-AuNps was found to be greater than pristine MWCNT (I_D/I_G - 0.715). To mention specifically, the obtained I_D/I_G values such as 0.753, 0.780 and 0.849 indicates the successful functionalization of –COOH on MWCNT, PAMAM (G3) on MWCNT-COOH/OH and immobilization of gold nanoparticles on MWCNT-PAMAM (G3)-AuNps respectively.

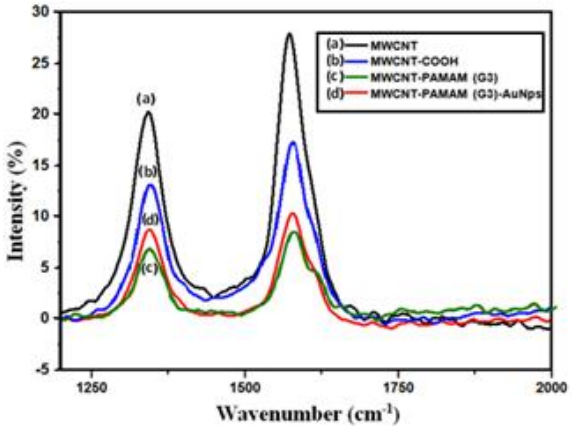

Fig. 2. Raman spectra of (a) MWCNT, (b) MWCNT-COOH, (c) MWCNT-PAMAM (G3) and (d) MWCNT-PAMAM (G3)-AuNps

Field Emission Scanning Electron Microscopy (FESEM) and High Resolution Transmission Electron Microscopy (HR-TEM) Studies

The surface morphology of the nanohybrids was inspected by field emission scanning electron microscopy and High Resolution Transmission Electron microscopy. The FESEM image of pristine MWCNT appeared as smooth surface long entangled tubes or bundles (**Fig. 3(a)**). While, oxidized MWCNT (**Fig. 3(b)**) appeared as rough surface tubes or bundles and this attributed to the existence of functional groups (COOH/OH) on their surface. The appearance of the surface functional groups on MWCNTs also accounted for repulsion between them and it caused well separation (debundeling) of MWCNTs which was strongly evident from the FESEM image. In addition to that, MWCNT-COOH/OH did not display considerable structural disruption possibly accounted for mild oxidizing reaction condition [**40, 41**]. Subsequent functionalization with PAMAM (G3) dendrimer on MWCNT-COOH/OH (**Fig. 3(c)**), the FESEM image revealed the untangled (debundled) MWCNT tubular

structure [**42**] due to the presence of greater quantum of functional groups (both –COOH/OH and PAMAM dendrimer) on the surface of MWCNT-PAMAM (G3) which could probably destruct the van der Waals forces acting between them [**43**]. Further, the FESEM image also revealed the coverage of white patches which possibly symbolized the successful functionalization of PAMAM (G3) dendrimer on MWCNT-COOH/OH. The FESEM image of MWCNT-PAMAM (G3)-AuNps (**Fig. 3(d)**), showed the presence of uniformly distributed white/ back dots which indicates the successful deposition of AuNps on the matrix of MWCT-PAMAM (G3). Similarly, the HRTEM image of MWCNT-PAMAM (G3)-AuNps (**Fig. 3(e)**) also displayed untangled/debundled rough surfaced tubular structure as well as the coverage of white patches with presence of dense dark dots which in turn provided a strong evidence for functionalization of PAMAM (G3) dendrimer molecule as well as deposition of gold nanoparticle in the conducting hybrid

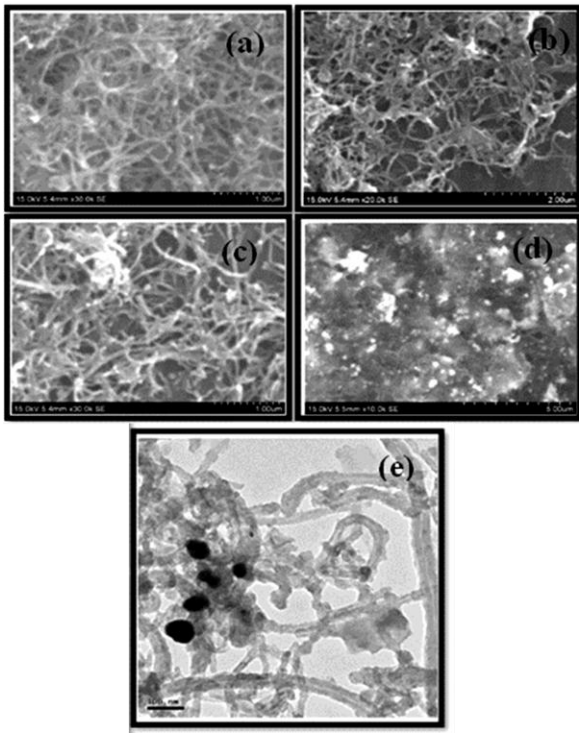

Fig. 3. FESEM images of (a) MWCNT, (b) MWCNT-COOH, (c) MWCNT-PAMAM (G3), (d) MWCNT-PAMAM (G3)-AuNps and (e) HRTEM image of MWCNT-PAMAM (G3)-AuNps

Electrochemistry of GCE-MWCNT-PAMAM (G3)-AuNps

The electrochemical nature of the three fabricated electrodes namely GCE-MWCNT, GCE-MWCNT-PAMAM (G3) and GCE-MWCNT-PAMAM (G3)-AuNps was preliminarily investigated by cyclic voltammetry under identical conditions using 0.5M H_2SO_4 (pH 1.54) as supporting electrolyte. **Fig. 4(A)** showed the typical cyclic voltammograms recorded at the scan rate of 50 mV s^{-1} obtained for GC-MWCNT (a), GC-MWCNT-PAMAM (G3) (b) and GC-MWCNT-PAMAM (G3)-AuNps (c) electrodes respectively. The comparative study of these three voltammograms reveals that the voltammogram of GC-MWCNT-PAMAM (G3)-AuNps electrode alone produced a single well defined cathodic peak at ~1.025 V than with GC-MWCNT and GC-MWCNT-PAMAM (G3) electrodes. From the observations, it can be concluded that the enhanced peak current noticed in GC-MWCNT-PAMAM (G3)-AuNps electrode may be as a result of efficient conducting nanohybrid. That is, it is the effect of synergistic contribution of MWCNT, PAMAM (G3) dendrimer and gold nanoparticles.

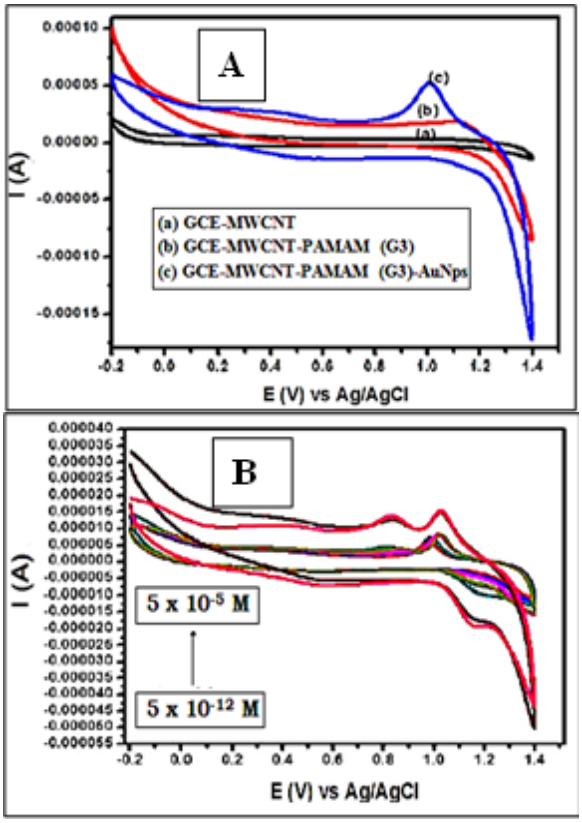

Fig. 4. (A) Cyclic voltammogram of (a) GCE-MWCNT (b) GCE-MWCNT-PAMAM (G3) and (c) GCE-MWCNT-PAMAM (G3)-AuNps under 0.5M H_2SO_4 supporting electrolyte, υ = 50 mVs^{-1}. (B) Influence of Capecitabine concentration from 5 x 10^{-12} M to 5x 10^{-5} M under 0.5M H_2SO_4 supporting electrolyte, υ = 50 mVs^{-1}

Particularly, the availability of extensive surface area on MWCNT leads to attract more amounts of PAMAM (G3) dendrimer molecules on its surface via, functionalization. Parallely, the intense functionalization of PAMAM (G3) dendrimer occurred on MWCNT have provided more number of surface $–NH_2$ groups which in turn enabled to attract more number of gold nanoparticles on the surface of MWCNT-PAMAM (G3) via entrapment process and thus produced excellent conducting nanohybrid material. Hence, coating of this excellent nanohybrid on GC electrode is totally responsible for production of enhanced cathodic peak. The peak observed at

~1.025 V can be ascribed to the reduction of gold corresponding to the reaction equation [**44**].

$$Au(OH) + e^- \longrightarrow Au + OH^-$$

The electro-conductive efficiency of these three fabricated electrodes was observed in the order as follows: GCE-MWCNT-PAMAM (G3)-AuNps > GCE-MWCNT-PAMAM (G3) > GCE-MWCNT. In order to examine the real time application, the newly designed electrode was chosen for further studies i.e., it was demonstrated for sensing and detection of trace/negligible quantity of Capecitabine drug.

Determination of trace quantity of Capecitabine using GC-MWCNT-PAMAM (G3)-AuNps electrode

The voltammetric behaviour of GC-MWCNT-PAMAM (G3)-AuNps electrode in the presence of Capecitabine drug in a supporting electrolyte of 0.5 M H_2SO_4 (pH 1.54) under the scan rate of 50 mV s^{-1} displayed two cathodic peaks at ~0.835 V and ~1.025 V (**Fig. 4(B)**). The peak noticed at ~0.835 V corresponds to the reduction of Capecitabine drug, whereas the peak observed at ~1.025 V was due to reduction of gold. On reverse scan, single anodic peak appeared due to oxidation of gold and revealed that the reduction of Capecitabine is a totally irreversible electrode process [**44**]. This observation demonstrated that the GC-MWCNT-PAMAM (G3)-AuNps electrode are efficient in sensing/detecting the Capecitabine drug even at lower concentration range.Further, the effect of Capecitabine concentration on the cathodic peak current was studied by varying the drug concentration from 5 x 10^{-12} M to 5 x 10^{-5} M at the scan rate of 50 mVs^{-1}. It is evident from the obtained voltammogram that with the subsequent increase in drug concentration, the reductive peak current enhanced accordingly and signifies excellent electro-conductivity of GC-MWCNT-PAMAM (G3)-AuNps electrode. Remarkable increase in peak current with increase in drug concentration under identical conditions suggested the evidence for better electron transfers efficiency of GC-MWCNT-PAMAM (G3)-AuNps electrode even at low Capecitabine concentration.

Effect of scan rate

In order to obtain the electrochemical mechanism of Capecitabine reduction, the effect of scan rate was investigated by varying the scan rate from 10 mV s^{-1} to 100 mV s^{-1} at a fixed lower concentration of Capecitabine of 5x10^{-12} M using 0.5 M H_2SO_4 as supporting electrolyte at GCE-PAMAM (G3)-AuNps [**Fig. 5(A)**]. From the obtained voltammogram it is evident that with subsequent scans, the cathodic peak current (I_{pc}) for the reduction of Capecitabine was found to increase gradually. These observations demonstrated that GC-PAMAM (G3)-AuNps electrode was stable, active and efficient in detecting the drug at lower concentration i.e., 5 x 10^{-12} M even under lower potential scan rate. Therefore, it is noteworthy to mention here that, the fabricated electrode GCE-MWCNT-PAMAM (G3)-AuNps showed stronger evidence (i) for detection of Capecitabine drug in lower concentration and (ii) at the same time sensing/ detecting at lower potentials. A plot of cathodic peak current (I_{pc}) and scan rate (υ) showed a linear association among them with correlation coefficient of 0.9969 [**Fig. 5(B)**] which in turn suggested that the reduction of Capecitabine have proceeded adsorption (surface controlled) process on GCE-PAMAM (G3)-AuNps electrode [**45**]. Similarly, a linear behaviour was observed between cathodic peak current (I_{pc}) and square root of scan rate ($\upsilon^{1/2}$) [**Fig. 5(C)**] with correlation coefficient of 0.9982, suggesting that the diffusion controlled mass transport of Capecitabine drug occurred towards the electrode surface [**46**].

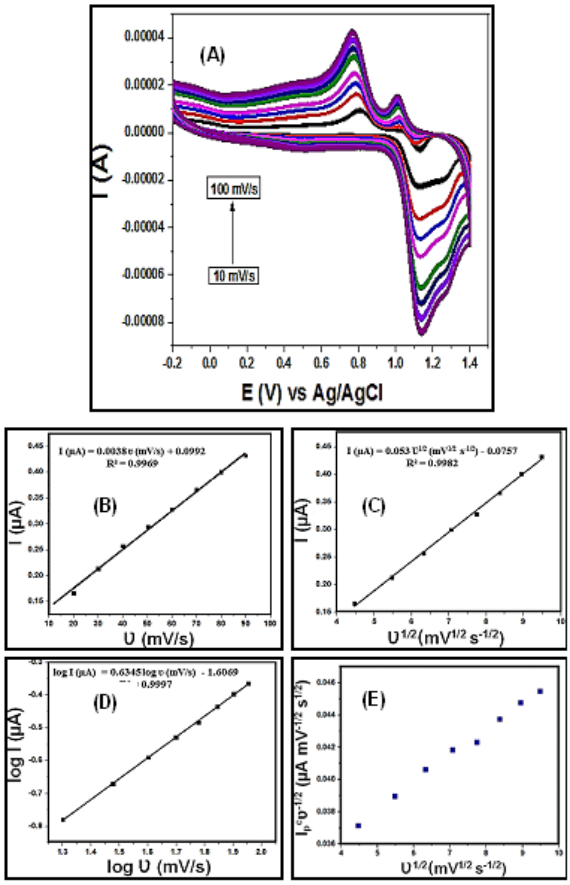

Fig. 5. Influence of scan rate, (A) Cyclic voltammograms of 5 x 10^{-12} M Capecitabine on GCE-MWCNT-PAMAM (G3)-AuNps with varying scan rates from 10 to 100 mVs^{-1} and 0.5 M H_2SO_4 as supporting electrolyte (pH 1.54), (B) Linear dependence of the reduction peak current on scan rates, (C) Linear dependence of the reduction peak current on the square root of scan rates, (D) Linear dependence of the logarithm of peak current on the logarithm of scan rates and (E) plot of cathodic current function with square root of scan rates.

A linear relationship was noticed between logarithm of cathodic peak currents (log I_{pc}) and logarithm of scan rate (log υ) [**Fig. 5(D)**] with the

slope value of 0.6345 and expressed by the equation. Since the slope value lies in between 0.5 (pure diffusion controlled) and 1.0 (pure adsorption controlled) [**47**] the reduction of Capecitabine occurred on the GC-MWCNT-PAMAM (G3)-AuNps electrode surface can be concluded to be under mixed adsorption-diffusion controlled process as rate determining factors. According to this phenomenon, the cathodic peak current for the reduction of Capecitabine was observed due to the contribution of both (i) drug molecule adsorbed on the electrode surface and (ii) diffusion of drug molecules towards electrode surface [**48,49**]. **Fig. 5(E)** showed a gradual increase in cathodic current function ($I_p^c \upsilon^{-1/2}$) with increase in square root of scan rate ($\upsilon^{1/2}$), highlighting the Electrochemical-Chemical (EC) mechanism of Capecitabine reduction on GCE-MWCNT-PAMAM (G3)-AuNps. In other words, EC mechanism involves initial charge transfer reaction and subsequent irreversible chemical reaction [50,51].

Reaction Mechanism

The mechanism of Capecitabine reduction can be suggested based on the cyclic voltammetry analysis as two-electron two-proton process. A plausible reaction mechanism of 5'-deoxy-5-fluoro-N-[(pentyloxy) carbonyl]-cytidine (Capecitabine) reduction to 5`-deoxy-5-flurocytidine (5`-DFCR) was illustrated in Fig. 6. Probably, the carbonyl group of amide bond present in drug is susceptible for reduction, resulting in amide bond breakage and analogous studies are already reported [**35**].

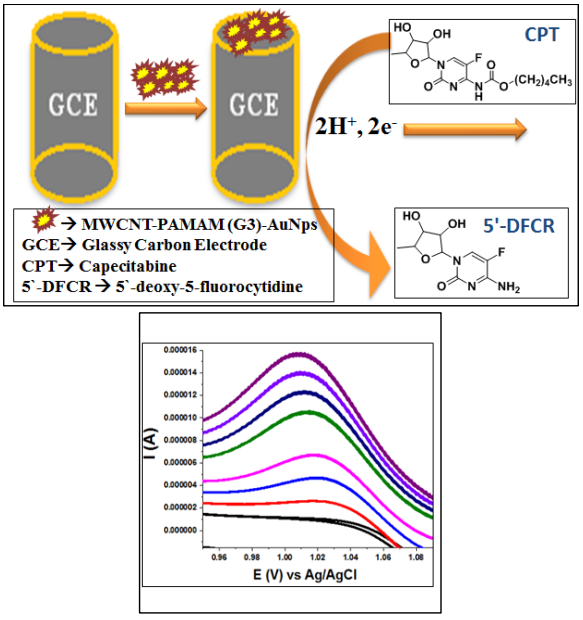

Fig. 6. Mechanism of Capecitabine reduction on GCE modified MWCNT-PAMAM (G3)-AuNps with their CV.

Conclusion

In this study, an efficient electrochemically active nanohybrid namely MWCNT-PAMAM (G3)-AuNps was synthesized by integration of three different nanomaterials like MWCNT, dendrimer and gold nanoparticles. Using this nanohybrid stable and efficient nano-electrode viz., GCE-MWCNT-PAMAM (G3)-AuNps was fabricated and demonstrated successfully for sensing/ detection of trace quantity of Capecitabine drug by cyclic voltammetry technique in the presence of H_2SO_4 (pH 1.54) as supporting electrolyte. Capecitabine showed a single cathodic peak with the absence of anodic peak on reverse scan, signifying the irreversible electron transfer mechanism of drug reduction at electrode process. The effect of potential scan rate on current peak current emphasized the contribution of both diffusion and adsorption controlled phenomenon for the reduction of Capecitabine. The influence of Capecitabine concentration on peak current was also addressed. The reaction mechanism was proposed as irreversible electrochemical-chemical (EC) process of two-proton two-electron reduction reaction of Capecitabine. The excellent electrocatalytic behavior of the fabricated electrode was attributed to three different smart materials viz., MWCNT, PAMAM (G3) dendrimer and AuNps. To conclude, the fabricated nano-electrode viz., GCE-MWCNT-PAMAM (G3)-AuNps has effectively sensed/ detected the trace quantity of Capecitabine drug (5 picomolar) under lower potentials and thus this nano-electrode can be recommended for real time application i.e., detection/sensing of negligible quantity of Capecitabine drug both in pharmaceutical quality control and biomedical laboratories.

Acknowledgements

We wish to thank NCNSNT, University of Madras, for rendering characterisation facilities.

References

1. Heidelberger, C.; Chaudhuari, N. K.; Daneberg, P.; Mooreh, D.; Griesbach, L.; Duschinsky, K.; Schnitzer, R. J.; Pleven, E. *Nature*. 1957, *179*, 663.
2. O'Shaughnessy, J. A.; Kaufmann, M.; Siedentopf, F.; Dalivoust, P.; Debled, M.; Robert, N. J.; Nadia Harbeck, N. *Oncologist*. 2012, *17*, 476.
3. McKendrick, K.; Coutsouvelis, J. *Expert Opin Pharmacother*. 2005,*6*, 1231.
4. Dyar, S.; Moreno-Aspitia, A. *Breast Cancer (Auckl)*. 2011; *5*, 239.
5. Schüller, J.; Cassidy, J.; Dumont, E.; Roos, B.; Durston, S.; Banken, L.; Utoh, M.; Mori, K.; Weidekamm, E.; Reigner, B. *Cancer Chemother. Pharmacol.*, 2000, *45*, 291.
6. Miwa, M.; Ura, M.; Nishida, M.; Sawada, N.; Ishikawa, T.; Mori, K.; Shimma, N.; Umeda, I.; Ishitsuka, H. *Eur J Cancer* 1998, *34*, 1274.
7. Couch, L. S. B.; Groteluschen, D. l.; Stewart, J.A.; Mulkerin, D. L. *Clin Colorectal Cancer*. 2003, *3*, 121.
8. Fontanella, C.; Aita, M.; Cinausero, M.; Aprile, G.; Baldin, M. G.; Dusi, V.; Lestuzzi, C.; Fasola G.; Puglisi, F. *Onco Targets Ther*. 2014, *7*, 1783.
9. Sideris, S.; Loizidou, A.; Georgala, A.; Lebrun, F.; Gil, T.; Awada. P.; Piccart, P.; Cardoso, F. *Acta Clin Belg*. 2013, *68*,135.
10. Yokokawa, T.; Kawakami, K.; Mae, Y.; Sugita, K.; Watanabe, H.; Suzuki, K.; Suenaga, M.; Mizunuma, N.; Yamaguchi, T.; Hama, T. *Ann Pharmacother*. 2015, *49*, 1120.

11. Nikolic-Tomasevic, Z.; Jelic, S.; Cassidy, J.; Filipovic-Ljeskovic, I.; Tomasevic, Z. *Cancer Chemother Pharmacol*. 2005, *6*, 594.
12. Piórkowska, E.; Kaza, M.; Fitatiuk, J.; Szlaska, I.; Pawinski, T.; Rudzki, P J. *Pharmazie*, 2014, *69*, 500.
13. Deenen, M. J.; Rosing, H.; Hillebrand, M. J.; Schellens, J. H.; Beijnen, J. H. *J Chromatogr B Analyt Technol Biomed Life Sci.* 2013, *30*, 913.
14. Montange, D.; Bérard, M.; Demarchi, M.; Muret, P.; Piédoux, S.; Kantelip, J. P.; Royer, B. *J Mass Spectrom.* 2010, *45*, 670.
15. Vainchtein, L. D.; Rosing, H.; Schellens, J. H.; Beijnen, J. H. *Biomed Chromatogr*. 2010, *24*, 374.
16. Deng, P.; Ji, C.; Dai, X.; Zhong, D.; Ding, L.; Chen, X. *J Chromatogr B Analyt Technol Biomed Life Sci.* 2015, *989*, 71.
17. Wang, X.; Zheng, K.; Feng, X.; Xu, C.; Song, W. *Sens Actuators B Chem.* 2015, *219*, 361.
18. Pattar, V. P.; Nandibewoor, S. T. *J Taibah Univ Sci*. 2016, *10*, 92.
19. Badawy, W. A.; El-Ries, M. A.; Mahdi, I. M. *Talanta*. 2010, *82*, 106.
20. Gupta, V. K.; Jain, R.; Agarwal, S.; Mishra, R.; Dwivedi, A. *Anal Bioche.* 2011, *410*, 266.
21. Gowda, J. I.; Nandibewoor, S. T. *Asian J Pharm Sci*. 2014, *9*, 42.
22. Kurbanoglu, S.; Dogan-Topal, B.; Uslu, B.; Can, A.; Ozkan, S. A. *Electroanalysis.* 2013, *25*, 1473.
23. Iijima, S. *Nature*. 1991, *354*, 56.
24. Zhao, Q.; Gan, Z.; Zhuang, Q. *Electroanalysis.* 2004,*14*, 1609.
25. Cao, Q.; Rogers, J. A. *Nano Res.* 2008, *1*, 259.
26. Zhang, W.; Zhang, Z.; Zhang, Y. *Nanoscale Res Lett.* 2011, *6*, 555.
27. Liu, Z.; Yang, K.; Lee, S. T. *J.Mater.Chem.* 2011, *21*, 586.
28. Murugan, E.; Vimala, G. *J. Phys. Chem. C*. 2011, *115*, 19897.
29. Thakur, V. K.; Thakur, M. K. Chemical Functionalization of Carbon Nanomaterials: Chemistry and Applications; CRC Press, 2015, pp 592-593.
30. Caminade, A. M.; Majoral, J. P. *Chem Soc Rev*. 2010, *39*, 2034.
31. Tomalia, D.A.; Baker, H.; Dewald, J.; Hall, M.; Kallos, G.; Martin, S.; Roeck, J.; Ryder J.; Smith, P. *Polym J.* 1985, *17*, 117.
32. Sutriyo; Mutalib, A.; Ristaniah; Anwar, E.; Radji, M.; Pujiyanto, A.; Purnamasari, P.; Joshita, D.; Adang, H. G. *Macromol Symp*. 2015, *353*, 96.
33. Zhang, Y,; Liu, X.; Li, L., Guo, Z.; Xue, Z.; Lu, Z. *Anal. Methods.* 2016, *8*, 2218.
34. Niu, Y.; He, J.; Li, Y.; Zhao, Y.; Xia, C.; Yuan, G.; Zhang, L.; Zhang, Y.; Yu, C. *Microchim Acta.* 2016, *183*, 2337
35. Kalanur, S. S.; Seetharamappa, J.; Mamatha, G. P.; Hadagali, M. D.; Kandagal, P.B. *Int. J. Electrochem.Sci.*, 2008, *3*, 756.
36. Shanmugharaj, A. M.; Bae, J. H.; Lee, K . Y.; Noh, W. H.; Lee S. H.; Ryu, S. H. *Compos. Sci. Technol.* 2007, *67*, 1813.
37. Pan, B.; Cui, D.; Xu, P.; Ozkan, C.; Feng, G.; Ozkan, M.; Huang, T.; Chu, B.; Li, Q.; He, R.; Hu, G. *Nanotechnology* 2009, *20*, 9.
38. Filho, A. G. S.; Jorio, A.; Samsonidze, G. G.; Dresselhaus, G.; Saito, R.; Dresselhaus, M. S. *Nanotechnology*. 2003, *14*, 1130.
39. Neelgund, G. M.; Oki, A.; Luo, Z. Colloids Surf B Biointerfaces. 2012, *100*, 215
40. Buang, N. A.; Fadil, F.; Majid, Z. A.; Shahir, S. *Dig J Nanomater Biostruct*. 2012, *7*, 33.
41. Mohammed, M. R.; Haider, A. J.; Ahmed, D. S. *Eng. &Tech.J.* 2014, *32*, 427.
42. Murugan, E.; Vimala, G. *J Colloid Interface Sci.* 2011, *357*, 354.
43. Neelgund, G. M.; Oki, A. *Appl Catal B.* 2011, *110*, 99.
44. Zhang, W.; Bas, A. D.; Ghali, E.; Choi, Y. *Trans. Nonferrous Met. Soc. China.* 2015, *25*, 2037.
45. Ghoneim, M. M.; Abdel-Azzem, M. K.; El-Desoky, H. S.; Ghoneim, A. M.; Khattab, A. E. *J. Braz. Chem.* Soc. 2014, *25*, 1407.
46. Bard, A.J.; Faulker, L.R. Electrochemical Methods: Fundamentals and Applications; John Wiley: New York, 2002.
47. Batchelor-McAuley, C.; Goncalves, L. M.; Xiong, L.; Barros, A. A.; Richard G. Compton, R. G. *Chem.Commun.* 2010, *46*, 9037.
48. Gosser, D. K. Cyclic voltammetry: simulation and analysis of reaction mechanisms; Wiley: USA, 1993.
49. Laviron, E.; Roullier, L.; Degrand, C.; *J. Electroanal. Chem.* 1980, *112*, 11.
50. Gupta, R.; Guin, S. K.; Aggarwal, S. K. *RSC Adv*. 2012, *2*, 1810.
51. Shamsipur, M.; Najafi, M.; Hosseini, M. R. M. *Bioelectrochemistry.* 2010, *77*, 120.

